THE JOURNAL OF PHYSICAL CHEMISTRY C

Article

pubs.acs.org/JPCC

Site-Specific Assembly of Fullerene Nanorings Guided by Two-Dimensional Gold Clusters

Yang-chun Xie,[†,∥] Mahroo Rokni Fard,[†,∥] Dogan Kaya,[†,∥] Deliang Bao,[‡,§,∥] Richard E. Palmer,[†] Shixuan Du,[*,‡] and Quanmin Guo[*,†]

[†]Nanoscale Physics Research Laboratory, School of Physics and Astronomy, University of Birmingham, Birmingham B15 2TT, United Kingdom

[‡]Institute of Physics, Chinese Academy of Sciences, Beijing 100190, China

[§]The University of Chinese Academy of Sciences, Beijing 100049, China

Supporting Information

ABSTRACT: Molecules can self-assemble rather easily into straight one-dimensional wires via covalent or noncovalent bonding. To organize molecules into cyclic structures such as rings or loops where the number of molecules forming each structure is accurately controlled is a much more challenging task. Here we demonstrate the construction of fullerene nanorings on the (111) plane of gold using single-atomic-layer-high gold islands as the seeding agent. C_{60} molecules are trapped by the step edges of the seeding Au island leading to the formation of molecular rings. The smallest ring consists of six C_{60} molecules encircling 19 Au atoms. Scanning tunneling microscopy imaging reveals that the rings are formed at specific locations on the reconstructed Au(111) surface with the diameter of the ring controlled by the size of the gold island. Molecular mechanics modeling provides a detailed understanding of the relationship between the number of molecules in the ring and the number of gold atoms within the Au island.

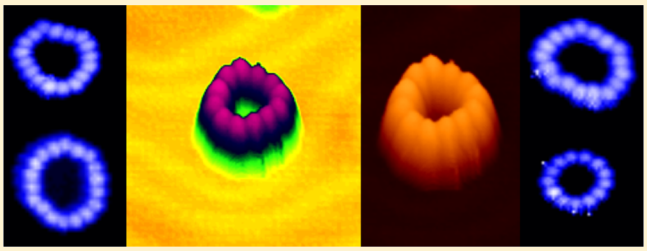

INTRODUCTION

The first manmade nanoring on a solid surface was created by manipulation of iron atoms on a copper surface using a scanning tunnelling microscope.[1] The electron charge density oscillation within such a ring follows closely the prediction of quantum mechanics, and for this reason this type of ring became known as a quantum corral. This pioneering work has inspired continued efforts to find new and more versatile routes to creating quantum corrals by means of supramolecular chemistry[2] or by directed surface assembly.[3] The self-assembly approach such as that used by Klappenberger et al.[3] is much more efficient than the original atom manipulation method[1] and is hence more promising for practical mass production. Self-assembly works well with a range of different materials such as colloids[4] and metal nanoparticles,[5] as well as molecules.[6] The assembly process can be controlled rather accurately by altering the forces among the elemental blocks in the system[7−14] or, as demonstrated recently, by changing the geometric shape of the building blocks.[15] Nanostructures achieved by molecular self-assembly on surfaces are usually in the form of large extended periodic structures of a repeating unit. To make isolated nanorings, one can choose a template to confine the growth of interesting structures to specific locations. Here we report the formation of fullerene nanorings on gold surfaces where two-dimensional Au clusters are used as the nucleation centers. The fullerene nanorings resemble those formed naturally in photosynthetic complexes by *Rhodospirillum photometricum* cells.[16] Because fullerenes are active ingredient in organic solar cells, the formation of rings may prove to be a significant step in producing solar cells with a structure that mimics that of photosynthetic bacteria.

METHODS

Experimental Methods. Experiments were performed in an ultrahigh vacuum (UHV) system equipped for variable temperature scanning tunneling microscopy.[17−20] The gold sample was a thin film ∼300 nm thick prepared by physical vapor deposition onto freshly cleaved highly oriented pyrolitic graphite (HOPG). The Au film was cleaned in the UHV chamber by many cycles of Ar+ ion sputtering and thermal annealing to 1000 K. C_{60} molecules were deposited onto the sample using a homemade evaporation source. Au atom deposition is performed using a Createc high-temperature effusion cell. An Omicron VT-STM was used for microscopic imaging of all structures. Electrochemically etched tungsten tips were used after initial heat treatment. Image processing was conducted using Image-SXM and ImageJ.

Computational Methods. The molecule mechanics (MM) method is performed to simulate the Au−C_{60} complex configurations. The COMPASS force field is employed to

Received: March 17, 2016
Revised: April 29, 2016
Published: May 6, 2016

DOI: 10.1021/acs.jpcc.6b02798
J. Phys. Chem. C 2016, 120, 10975−10981

investigate the interactions between C_{60} molecules and Au islands. The force field type for Au and C element is Au_m and c3a, respectively. As for six and seven C_{60} molecules, the model is built with a 16 × 17 Au(111) surface containing three atomic layers, with the adsorbing Au island and C_{60} molecules on one side of the slab. For more than seven C_{60} molecules, the substrate expands to a 20 × 20 unit cell. The atoms in Au clusters are located at the face-centered cubic (fcc) region on the Au(111) surface. The models are not periodic. In relaxation, the slabs are all fixed, while all C atoms in C_{60} molecules and Au atoms in clusters are fully relaxed until the system energy gradient is lower than 1×10^{-4} kcal/mol.

The density functional theory (DFT) calculation is also performed with Perdew–Burke–Ernzerhof (PBE) flavor of the generalized gradient approximation (GGA) in all-electron plane-wave formulation in the VASP code. An energy cutoff of 400 eV is used. The C_{60}–Au edge system is modeled by a 6 × 10 Au(111) surface containing three atomic layers of Au and a C_{60} molecule adsorbed on one side of the slab. Some Au atoms in the layer closed to C_{60} molecule is taken off to simulate an edge on the surface. Au atoms in the bottom two layers are fixed, while the edge layer and C_{60} molecule are relaxed until the atomic forces are lower than 0.02 eV/Å. The van der Waals (vdW) interaction is considered with the DFT-D2 method of Grimme in our calculation.

RESULTS AND DISCUSSION

Figure 1 illustrates the basic procedure implemented for the assembly of C_{60} nanorings. First, Au atoms are deposited onto

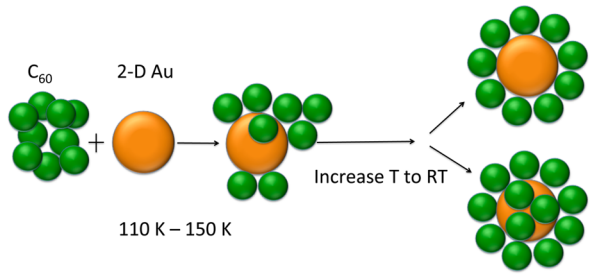

Figure 1. Schematic of self-assembly of C_{60}–Au complex structures. Green circles represent C_{60} molecules; the large orange circle represents a two-dimensional Au island. The Au island is preformed by deposition of Au atoms onto Au(111) in the temperature range of 110–150 K. Subsequent deposition of C_{60} molecules conducted between 110 and 150 K gives rise to C_{60}-decorated Au islands. By warming up to room temperature, two types of well-defined structures are formed: (i) a C_{60} nanoring around the Au island and (ii) a compact island of C_{60} with some molecules sitting above the Au island.

the Au(111) substrate which is kept at temperatures between 110 and 150 K, giving rise to small single-atomic-layer-high Au islands. C_{60} molecules are subsequently deposited onto the same surface while the sample remains at <150 K. The step edges of the preformed Au islands thus become decorated by the C_{60} molecules. The temperature of the sample is then increased gradually to room temperature to allow self-regulated growth and ripening of stable structures.

The Au(111) surface has a well-known herringbone-type of reconstruction which is characterized by a two-dimensional network of dislocations.[21,22] The dislocation, analogous to the edge dislocation found in three-dimensional materials, is formed by the termination of an atomic row.[23,24] Figure 2a

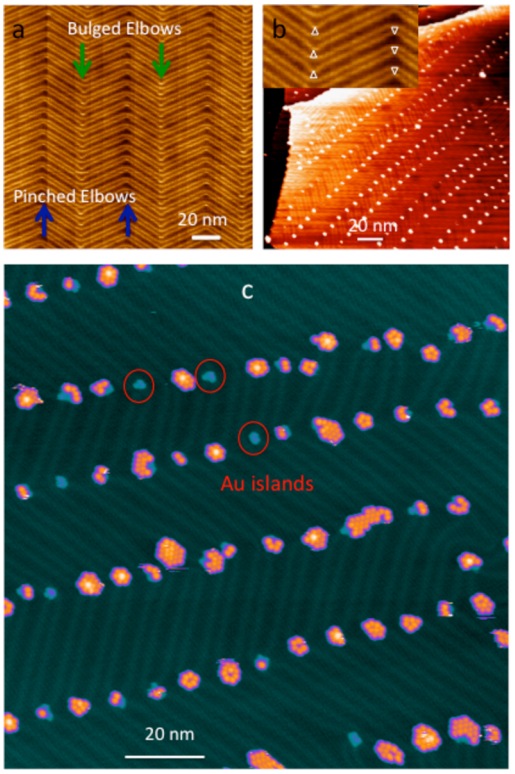

Figure 2. Formation of C_{60}–Au complex structures at low temperatures. (a) STM image of the clean herringbone-reconstructed Au(111) surface. (b) Small Au islands formed at the elbow sites after deposition of 0.03 ML of Au at 120 K. Triangles drawn in the inset show the locations of the Au islands. (c) Structures formed after adding 0.015 ML of C_{60} at 150 K onto a surface having preformed Au islands. Red circles highlight a few bare Au islands with no C_{60} molecules attached.

shows a scanning tunneling microscopy (STM) image of the clean Au(111) surface revealing the pattern of the herringbone reconstruction and the presence of two types of elbow sites. Each elbow is associated with a defect. One side of the defect, where the extra row of Au atoms is located, is under compressive stress, and the opposite side is under tensile stress. The Au island nucleates at the defect and expands into the area under tensile stress. For the bulged elbow site, the Au island is thus found in the fcc domain, whereas the Au island is found in the hexagonal close-packed (hcp) domain at the pinched elbow site as shown in Figure 2b. The amount of gold atoms deposited in our study is low enough such that the Au island at the bulged elbow site does not spread into the neighboring hcp region, and the Au island at the pinched elbow site does not spread into the fcc region. When C_{60} molecules are deposited onto the surface at 110–150 K, they diffuse until they are captured by the preformed Au islands resulting in the formation of irregular C_{60}–Au complexes, as shown in Figure 2c. It can be seen that Au clusters are fully or partially surrounded by C_{60} molecules. The molecules appearing "bright" in the image are those sitting directly above the Au island. The location of the C_{60}–Au complex follows that of the preformed Au island: the C_{60}–Au complex is confined inside the fcc domain at the bulged elbow and inside the hcp domain at the pinched elbow, respectively.

The C_{60}–Au complex formed at 150 K as shown in Figure 2c is far from uniform in terms of both size and shape. The number of C_{60} molecules linked to a Au island ranges from 1 to

DOI: 10.1021/acs.jpcc.6b02798
J. Phys. Chem. C 2016, 120, 10975–10981

about 15 with an average value of ~6. With just 0.015 ML of C_{60} deposited, there is also a very small number of Au islands with no C_{60} molecules attached. When the temperature of the sample is raised, not much change is observed below 240 K. Above 240 K, major structural transformations take place involving atom/molecule transportation across the surface. Bare Au islands with no C_{60} attached are the least stable and the first to disappear. Au islands with only a small fraction of its step edges covered by C_{60} molecules are the next to disintegrate. The Au atoms released from the fragmentation of these Au islands are incorporated into other islands. Similarly, there are also C_{60} molecules diffusing on the surface, and they are ready to join nearby C_{60}–Au complexes.

In between 240 and 290 K, rapid exchange of Au atoms and C_{60} molecules among the C_{60}–Au complexes leads to the formation of two types of stable structures at room temperature, Figure 3. One type of stable structures takes the form of compact islands with an exact number of C_{60} molecules, known as magic number clusters; these were analyzed, and the results were reported in an earlier publication.[25] Here we will concentrate on the alternative type of C_{60}–Au complex: the C_{60} nanoring formed around step edges of the Au island. In Figure 3a, one can see full rings of C_{60} as well as partial rings. The full rings are mostly located in the fcc domains next to pinched elbow sites, with a small number also found inside the fcc domains far from the elbow sites. There are Au islands straddling the discommensuration lines such that part of the island is inside the fcc domain and the rest inside the hcp domain. For this type of Au islands, the step edges inside the fcc domain are decorated by C_{60} molecules, while the step edges within the hcp domain are exposed. Hence, partial molecular rings are formed around these Au islands. Figure 3b shows an image from a larger area demonstrating the spatial distribution of the two types of structures.

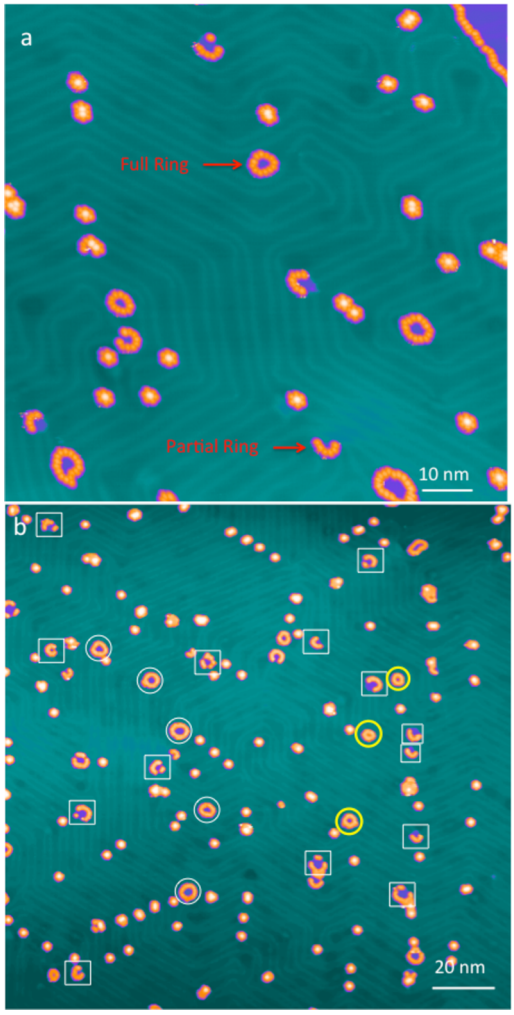

Figure 3. Formation of C_{60}–Au complex structures at room temperature. (a) STM image showing the presence of C_{60} nanorings at room temperature. (b) STM image from a larger area. Rings inside white circles consisting of ~15 molecules are formed around Au islands that already reached the maximum size allowed by the width of the fcc domain. Rings inside yellow circles are formed around Au islands yet to reach their maximum size. Structures inside white squares are partial rings formed around Au islands that straddle the hcp and fcc domains.

The structural transformation taking place between 240 and 290 K can be summarized in the following way. At the bulged elbow sites, small compact C_{60}–Au hybrid clusters are formed[25] in the fcc domain. The fcc domain next to the bulged elbow site is relatively narrow, ~1.2 nm, and this puts an upper limit on the size of the Au island. At the pinched elbow site, Au atoms and C_{60} molecules are able to move out of the hcp region as temperature is increased. They reassemble at the adjacent fcc region, giving rise to either a compact C_{60}–Au cluster or a C_{60} nanoring. The fcc region next to the pinched elbow is relatively wide, ~3.8 nm; hence, it can accommodate larger Au islands. In Figure 3b, the nanorings highlighted by white circles, consisting of about 15 molecules, are formed around Au islands that have grown to the maximum size allowed by the width of the fcc region next to the pinched elbow. The rings inside the yellow circles in Figure 3 have not yet reached the maximum allowed size.

Figure 4 shows examples of nanorings observed at room temperature. Due to the limited number of rings observed, it is not yet possible to produce a reliable size distribution for the rings. The majority of rings have 6–15 molecules. The shape of the ring does not simply depend on the number of C_{60} molecules ($N_{C_{60}}$); for example, with 11 C_{60} molecules, five different shaped rings are shown in Figure 4. It is likely that the shape of the ring also depends on the number of Au atoms (N_{Au}) enclosed. We performed molecular mechanics (MM) simulation to determine how the shape of the ring with a fixed number of molecules is influenced by the number of enclosed Au atoms.

We first examined the ring with six C_{60} molecules. Figure 5a,b shows that for such a ring, the optimized configuration is that each molecule sits next to one side of a hexagonal Au island consisting of 19 Au atoms. The distance between adjacent molecules is about 1 nm. For the carbon atoms that are in direct contact with the Au surface, the C–Au distance is about 0.25 nm. Both values are consistent with those reported previously for C_{60} molecules on the same Au(111) surface.[26] Figure 5c,d shows that for 11 C_{60} molecules, differently shaped rings can be formed. With 75 Au atoms in the gold island, the molecular ring takes a slightly distorted hexagonal shape (Figure 5c). With 64 Au atoms in the gold island, the same number, 11, of C_{60} molecules form an elongated ring, as shown in Figure 5d. Therefore, it can be stated that for a fixed number of C_{60} molecules the shape of the ring is determined by the number of Au atoms enclosed by the molecules.

DOI: 10.1021/acs.jpcc.6b02798
J. Phys. Chem. C 2016, 120, 10975–10981

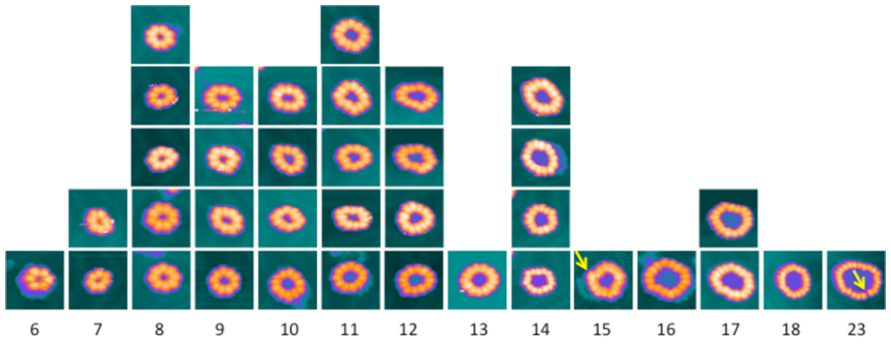

Figure 4. Examples of C_{60} nanorings observed at room temperature. The smallest ring consists of 6 molecules. The largest ring included in this set consists of 23 molecules (this is not the largest possible size). A ring with a given number of molecules, 11 for example, can have different shapes. The yellow arrow for the ring with 15 molecules points at a C_{60} molecule sitting further away from the step edge of the Au island than other molecules. The yellow arrow for the ring with 23 molecules points at a gap in the ring.

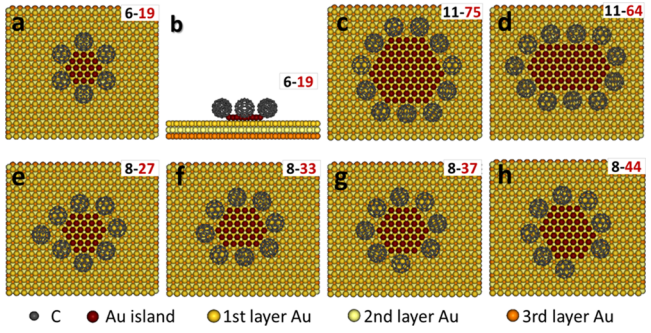

Figure 5. MM simulation of C_{60} nanoring formation. (a) Top view of a ring with six C_{60} molecules and 19 Au atoms. (b) Side view of the 6-C_{60} ring. (c) Ring with 11 molecules and 75 Au atoms. (d) Ring with 11 molecules but a reduced number, 64, of Au atoms. The changing number of Au atoms from 75 to 64 leads to a change in the geometry of the molecular ring. (e–h) The evolution of a nanoring configuration by changing the number of Au atoms in an 8-C_{60} ring. With 27 Au atoms, the perimeter of the Au island is not long enough to accommodate 8 molecules; hence, one of the molecules shoen in panel e is kept at a longer distance from the step edge. With 33 Au atoms, the perimeter of the Au island can support 8 C_{60} molecules. Adding more Au atoms to the island causes the formation of a gap in the molecular ring. The number in black at the top-right corner of each figure represents $N_{C_{60}}$, while the number in red represents N_{Au} in the gold island.

Under certain conditions, the Au island happens to be the "wrong size" such that the perimeter of the Au island cannot support an integral number of C_{60} molecules while keeping the C_{60}–C_{60} distance at 1 nm. In such cases, molecules line up along the step edges of the gold island maintaining the 1 nm distance between nearest-neighbor molecules. In Figure 5e, the perimeter of the Au island with 27 atoms can support 7 molecules but is too short for 8 molecules. When the eighth molecule is added to the existing structure, it stays at a larger distance from the step edge of the gold island. This kind of ring with a peripheral molecule has been observed in experiments, as shown in Figure 4 (ring with 15 molecules for example). The peripheral molecule is less strongly bound, and if this molecule moves away, a gap will occur in the molecular ring. Figure 5g,h shows 8-molecule rings with a gap. The Au island in Figure 5h is 14 atoms larger than that in Figure 5g, and consequently the gap is larger. In Figure 4, the STM image from the ring with 23 molecules shows such a gap which is not large enough to accommodate another molecule.

By assuming that the Au island always takes a hexagonal shape, which is a reasonable assumption for atomic islands on the (111) plane of fcc metals, we can determine N_{Au} rather precisely for a ring containing N–C_{60} molecules. The detailed method for calculating N_{Au} can be found in the Supporting Information. From experimental findings we know that the shape of the rings ranges from regular hexagons to elongated ones. Figure 6 shows the relationship between N_{Au} and $N_{C_{60}}$.

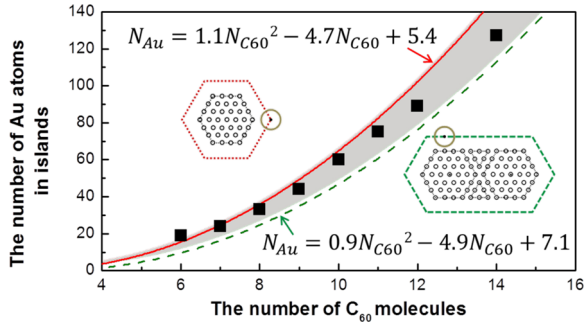

Figure 6. Relationship between the number of C_{60} molecules ($N_{C_{60}}$) and the number of Au atoms enclosed (N_{Au}). The red curve is based on the model with a regular hexagon, whereas the green curve is based on an elongated hexagon. The formulas producing the curves are displayed in the figure (see details in the Supporting Information).

The red curve corresponds to the result calculated for regular hexagonal rings, while the green dashed line corresponds to that of the elongated hexagonal island. The degree of elongation is limited by the stability of the metal island, which needs to minimize its total step energy. The shaded area between the two curves represents the possible values of N_{Au} and $N_{C_{60}}$ predicted by the model. For a number of experimentally observed rings consisting of 6–16 C_{60} molecules, the number of Au atoms in each ring has been evaluated using the relaxed model in Figures 5 and S3. The outcome is shown in Figure 6 with the filled squares. Therefore, the modeling provides a rather accurate evaluation of the number of gold atoms enclosed by the experimentally observed C_{60} rings. This overcomes the difficulty in directly counting the number atoms by STM.

The width of the fcc region next to a pinched elbow site is 3.8 nm. Experimental observations show that the rings are mostly confined within this fcc region. This suggests an upper limit for the number of Au atoms in the Au island is about 160.

DOI: 10.1021/acs.jpcc.6b02798
J. Phys. Chem. C 2016, 120, 10975–10981

Consequently, the C_{60} ring associated with such a Au island in the fcc region consists of no more than 15 molecules. Some rings are located far from the elbow site, in regions where the discommensuration lines are straight. The width of the fcc domain in such regions is 2.7 nm. The Au island in the fcc domain far from the elbows hence contains no more than ~110 Au atoms, and 13 molecules are expected to decorate the step edges of the gold island. As can be seen in Figure 3b, there exist local areas where fcc domains are larger than 3.8 nm because of the irregular bending of the discommensuration lines. This offers the opportunity to form a small number of molecular rings with more than 15 molecules.

Although the discommensuration lines tend to confine the Au island, they do not completely prevent the Au islands from growing to very large sizes. At room temperature (RT) and above, the Au island can expand by pushing further apart the discomensuration lines. Figure 7 shows an STM image of a Au

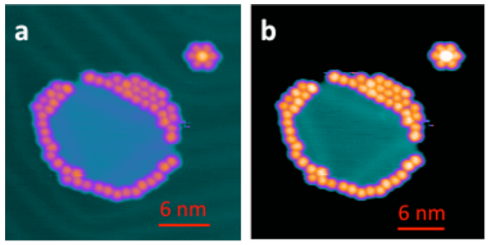

Figure 7. STM images of a Au island 13 nm across. (a) The island is formed as a result of increasing the sample temperature to ~400 K. The island is faceted, and its step edges consist of close-packed atoms. (b) Herringbone reconstruction takes place within the island. The image in panel b is the same as in panel a shown with enhanced contrast.

island which is 13 nm across. Au island of this size contains more than 1500 Au atoms and is clearly faceted. The usual herringbone reconstruction is observed within the island as revealed by the discommensuration lines[27,28] (Figure 7b). Because the amount of Au and C_{60} deposited on the surface is small, nearly all rings formed upon warming the sample to room temperature are confined between two pairs of discommensuartion lines. Each Au island is protected by a ring of molecules. However, when the temperature of the sample is further increased to 400 K, some rings are observed to fragment. The atoms and molecules released from the fragmentation are captured by other stable rings resulting in the formation of the extra large rings such as that shown in Figure 7.

The nanorings are stable at room temperature, as shown by sequential imaging of the same area over an extended period of time. Figure 8 shows STM images of six nanorings observed during a 5 min interval. The rings keep their form rather well even for rings with irregular shapes. One of the rings, Figure 8c,d, has a gap which is seen not to move with time. There might be edge diffusion of Au atoms occurring at the atomic level, but the overall morphology of the Au island is locked by the capping C_{60} molecules. The structure of the nanoring can be changed under certain conditions by the STM tip, for example, by using a larger bias voltage. Figure 8i shows an image of a ring with 15 molecules. Figure 8j shows an image of the same ring after scanning with an increased voltage of −2.46 V, which causes a clear change of the ring due to the

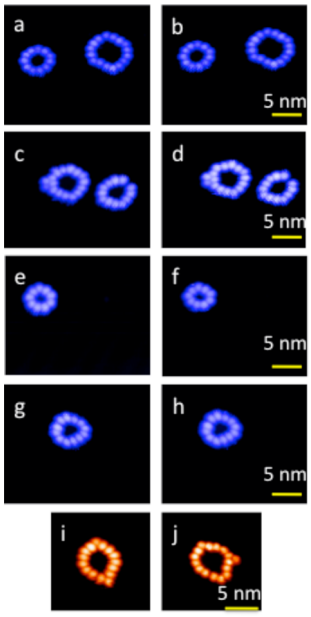

Figure 8. Stability of the nanorings at room temperature observed with the STM. Panels a, c, e, and g show the morphologies of the initial rings. Panels b, d, f, and h show the same rings after 5 min at room temperature. The noncircular shape of the rings allows any change to be easily identifiable. Panels i and j are STM images demonstrating the change of the ring due to the perturbation by the STM tip.

reorganization of C_{60} molecules and Au atoms. The ring has also captured an extra molecule.

In all the experiments performed so far, the nanorings were always found to coexist with compact magic number C_{60}–Au clusters. The fraction of the nanorings can be changed by altering the parameters used for deposition. For example, when more Au atoms are deposited to form relatively large bare gold clusters, the number of rings increases significantly. Figure 9a shows a STM image after 0.09 ML of Au and 0.17 ML of C_{60} are deposited at 150 K and the sample was warmed to room temperature. More than 50% of the features observed afterward are rings. This is much higher than ~5% of rings found in Figure 3 when smaller amounts of Au atoms and C_{60} molecules are deposited. Compact clusters can also be transformed into rings by adding more Au atoms, as demonstrated by the STM images in Figure 9b,c. In Figure 9b, the two clusters inside the white circles are identical clusters; each contains 14 C_{60} molecules. Four of the 14 molecules sit on the Au island. After the image in Figure 9b was collected, 0.003 ML of Au is deposited onto the sample at RT. Thus, some Au atoms join the 14-molecule clusters. The four bright molecules are found to jump down each of the Au islands and become part of the molecular ring surrounding the now enlarged Au islands, Figure 9c. During the structural transformation into rings, the cluster near the top-left corner mass-migrates collectively to a new location where the ring is formed. This collective migration suggests a cohesive interaction that keeps the atoms and molecules in a group as they travel on the surface. It is not likely that the whole cluster would move as an intact unit. Instead, the net displacement is accomplished probably by the movements of individual atoms or molecules in a loosely bound group.

DOI: 10.1021/acs.jpcc.6b02798
J. Phys. Chem. C 2016, 120, 10975−10981

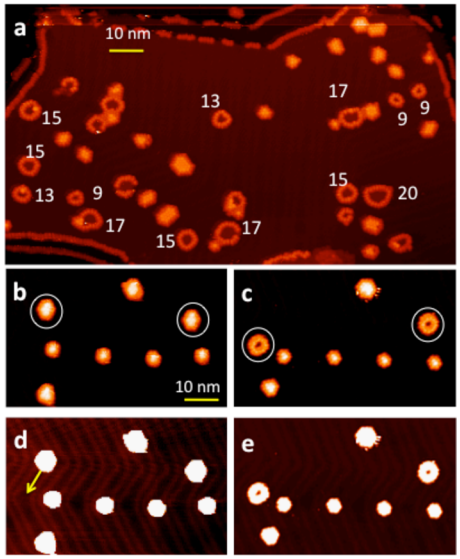

Figure 9. Scheme to increase the proportion of nanorings. (a) The fraction of nanorings is increased significantly when the amounts of Au and C_{60} deposited at 150 K are increased. The numbers next to the rings are the number of C_{60} molecules in the ring. Transformation from compact clusters to nanorings is demonstrated in panels b–e. In panel b, the two compact clusters within white circles are identical clusters each consisting of 14 C_{60} molecules; 4 of the 14 molecules sit directly above the Au island. These two clusters capture more Au atoms at room temperature and change into rings (c). The ring on the left is found at a different location from that of the initial compact cluster, indicating a collective migration of molecules and atoms during the formation of the ring. The yellow arrow in panel d shows the direction of displacement of the C_{60}–Au complex. The images in panels b and c are contrast enhanced and displaced in panels d and e, respectively, to show the locations of the C_{60}–Au complexes relative to the locations of the discommensuration lines.

SUMMARY

Molecular rings of C_{60}, resembling the structures formed naturally in photosynthetic complexes by *R. photometricum* cells, have been produced on the Au(111) surface. Both the size and location of the rings can be controlled by choosing suitable preparation procedures. Such molecular rings, encapsulating a metal or semiconductor core, have the potential to be developed into building blocks for new types of solar cells based on efficient charge transfer between the metal and the molecule[29] or high-density magnetic recording medium if the metal core is formed by magnetic materials.

ASSOCIATED CONTENT

Supporting Information

The Supporting Information is available free of charge on the ACS Publications website at DOI: 10.1021/acs.jpcc.6b02798.

Details regarding theoretical modeling (PDF)

AUTHOR INFORMATION

Corresponding Authors

*E-mail: Q.Guo@bham.ac.uk. Tel: +44 1214144657.
*E-mail: sxdu@iphy.ac.cn. Tel: +86 1082649823.

Author Contributions

‖Y.-C.X., M.R.F., D.K., and D.B. made equal contributions to this work.

Notes

The authors declare no competing financial interest.

ACKNOWLEDGMENTS

We thank the EPSRC of the United Kingdom for financial support.

REFERENCES

(1) Crommie, M. F.; Lutz, C. P.; Eigler, D. M. Confinement of electrons to quantum corrals on a metal surface. *Science* **1993**, *262*, 218–220.
(2) Kondratuk, D. V.; Perdigao, L. A.; Esmail, A. M. S.; O'Shea, J. N.; Beton, P. H.; Anderson, H. L. Supramolecular nesting of cyclic polymers. *Nat. Chem.* **2015**, *7*, 317–322.
(3) Klappenberger, F.; Kuhne, D.; Krenner, W.; Silanes, I.; Arnau, A.; Garcia de Abajo, F. J.; Klyatskaya, S.; Ruben, M.; Barth, J. V. Dichotomous array of chiral quantum corrals by self-assembled nanoporous Kagome network. *Nano Lett.* **2009**, *9*, 3509–3514.
(4) Kim, P. Y.; Oh, J. W.; Nam, J. M. Controlled co-assembly of nanoparticles and polymer into ultra long and continuous one-dimensional nanochains. *J. Am. Chem. Soc.* **2015**, *137*, 8030–8033.
(5) Gorgoll, R. M.; Tsubota, T.; Harano, K.; Nakamura, E. Cooperative self-assembly of gold nanoparticles on the hydrophobic surface of vesicles in water. *J. Am. Chem. Soc.* **2015**, *137*, 7568–7571.
(6) Heim, D.; Ecija, D.; Seufert, K.; Auwarter, W.; Aurisicchio, C.; Fabbro, C.; Bonifazi, D.; Barth, J. V. Self-assembly of flexible one-dimensional coordination polymers on metal surfaces. *J. Am. Chem. Soc.* **2010**, *132*, 6783–6790.
(7) Barth, J. V. Molecular architectonic on metal surfaces. *Annu. Rev. Phys. Chem.* **2007**, *58*, 375–407.
(8) Rosei, F.; Schunack, M.; Naitoh, Y.; Jiang, P.; Gourdon, A.; Lagsgaard, I.; Stensgaard, I.; Joachim, C.; Besenbacher, F. Properties of large organic molecules on metal surfaces. *Prog. Surf. Sci.* **2003**, *71*, 95–146.
(9) Theobald, J. A.; Oxtoby, N. S.; Phillips, M. A.; Champness, N. R.; Beton, P. H. Controlling molecular deposition and layer structure with supramolecular surface assemblies. *Nature (London, U. K.)* **2003**, *424*, 1029–1031.
(10) Pawin, G.; Wong, K.-L.; Kwon, K.-Y.; Bartels, L. A homomolecular porous network at a Cu(111) surface. *Science* **2006**, *313*, 961–962.
(11) Pivetta, M.; Pacchioni, G. E.; Schlickum, U.; Barth, J. V.; Brune, H. Formation of Fe cluster superlattice in a metal-organic quantum-box network. *Phys. Rev. Lett.* **2013**, *110*, 086102.
(12) Hanke, F.; Haq, S.; Raval, R.; Persson, M. Heat-to-connect: Surface commensurability directs organometallic one-dimensional self-assembly. *ACS Nano* **2011**, *5*, 9093–9103.
(13) Ecija, D.; Urgel, J. I.; Papageorgiou, A. C.; Joshi, S.; Auwarter, W.; Seitsonen, A. P.; Klyatskaya, S.; Ruben, M.; Barth, J. V. Five-vertex Archimedean surface tessellation by lanthanide-directed molecular self-assembly. *Proc. Natl. Acad. Sci. U. S. A.* **2013**, *110*, 6678–6681.
(14) Fernandez-Torrente, I.; Monturet, S.; Franke, K. J.; Fraxedas, J.; Lorente, N.; Pascual, J. I. Long-range repulsive interaction between molecules on a metal surface induced by charge transfer. *Phys. Rev. Lett.* **2007**, *99*, 176103.
(15) Lu, F.; Yager, K. G.; Zhang, Y.-G.; Xin, H.-L.; Gang, O. Superlattices assembled through shape-induced directional binding. *Nat. Commun.* **2015**, *6*, 6912.
(16) Scheuring, S.; Sturgis, J. N. Chromatic adaptation of photosynthetic membranes. *Science* **2005**, *309*, 484–487.
(17) Tang, L.; Xie, Y.-C.; Guo, Q. Complex orientational ordering of C_{60} molecules on Au(111). *J. Chem. Phys.* **2011**, *135*, 114702.
(18) Xie, Y.-C.; Tang, L.; Guo, Q. Underlayer growth of a nanoporous single atomic layer of gold. *J. Phys. Chem. C* **2012**, *116*, 5103–5109.
(19) Li, F. S.; Tang, L.; Zhou, W. C.; Guo, Q. Resolving the Au-adatom-alkanethiolate bonding site on Au(111) with domain

DOI: 10.1021/acs.jpcc.6b02798
J. Phys. Chem. C 2016, 120, 10975–10981

boundary imaging using high-resolution scanning tunneling microscopy. *J. Am. Chem. Soc.* **2010**, *132*, 13059−13063.
(20) Zhang, X.; Tang, L.; Guo, Q. Low temperature adsorption and growth of C_{60} monolayers on Au(111). *J. Phys. Chem. C* **2010**, *114*, 6433−6439.
(21) Scheuring, S.; Sturgis, J. N. Chromatic adaptation of photosynthetic membranes. *Science* **2005**, *309*, 484−487.
(22) Barth, J. V.; Brune, H.; Ertl, G.; Behm, R. Scanning tunneling microscopy observations on the reconstructed Au(111) surface. *Phys. Rev. B: Condens. Matter Mater. Phys.* **1990**, *42*, 9307−9318.
(23) Harten, U.; Lahee, A.; Toennies, J.; Woll, C. Observation of a soliton reconstruction of Au(111) by high-resolution helium-atom scattering. *Phys. Rev. Lett.* **1985**, *54*, 2619−2622.
(24) Chambliss, D. D.; Wilson, R. J.; Chiang, S. Nucleation of ordered Ni island arrays on Au(111) by surface-lattice dislocations. *Phys. Rev. Lett.* **1991**, *66*, 1721−1724.
(25) Xie, Y.-C.; Tang, L.; Guo, Q. Co-operative assembly of magic number C_{60}-Au complexes. *Phys. Rev. Lett.* **2013**, *111*, 186101.
(26) Wang, L.-L.; Cheng, H.-P. Density functional study of the adsorption of a C_{60} monolayer on Ag(111) and Au(111) surfaces. *Phys. Rev. B: Condens. Matter Mater. Phys.* **2004**, *69*, 165417.
(27) Sun, J.-T.; Gao, L.; He, X.-B.; Cheng, Z.-H.; Deng, Z.-T.; Lin, X.; Hu, H.; Du, S.-X.; Liu, F.; Gao, H.-J. Surface reconstruction transition of metals induced by molecular adsorption. *Phys. Rev. B: Condens. Matter Mater. Phys.* **2011**, *83*, 115419.
(28) El-Batanouny, M.; Burdick, S.; Martini, K.; Stancioff, P. Double sine-Gordon solitons- A model for misfit dislocations on the Au(111) reconstructed surface. *Phys. Rev. Lett.* **1987**, *58*, 2762−2765.
(29) Hunt, M. R. C.; Modesti, S.; Rudolf, P.; Palmer, R. E. Charge-transfer and structure in C_{60} adsorption on metal surfaces. *Phys. Rev. B: Condens. Matter Mater. Phys.* **1995**, *51*, 10039−10047.

DOI: 10.1021/acs.jpcc.6b02798
J. Phys. Chem. C 2016, 120, 10975−10981